AN ATLAS OF LEGENDRIAN KNOTS

WUTICHAI CHONGCHITMATE AND LENHARD NG

ABSTRACT. We present an atlas of Legendrian knots in standard contact three-space. This gives a conjectural Legendrian classification for all knots with arc index at most 9, including alternating knots through 7 crossings and nonalternating knots through 9 crossings. Our method involves a computer search of grid diagrams and applies to transverse knots as well. The atlas incorporates a number of new, small examples of phenomena such as transverse nonsimplicity and non-maximal non-destabilizable Legendrian knots, and gives rise to new infinite families of transversely nonsimple knots.

1. INTRODUCTION

A central problem in contact knot theory is the Legendrian and transverse classification problem: how to classify all Legendrian and transverse knots of a particular topological type in some contact 3-manifold. This is an interesting question even for the most basic case, $\mathbb{R}^3$ with the standard contact structure $\ker(dz - y\,dx)$. Legendrian and transverse knots have been classified in this case for a few families of knots, including the unknot [8], torus knots [10], and twist knots [13]. The classification problem for most other knots, however, including many "small" knots, is currently wide open.

In this paper, we present a conjectural Legendrian and transverse classification for all prime knots in $\mathbb{R}^3$ with arc index at most 9. This includes all prime knots with 7 or fewer crossings, all prime nonalternating knots with 9 or fewer crossings, and an assortment of other nonalternating knots. (One can use the prime classification to similarly classify composite knots, by the results of [12].) The classification is presented at the back end of this paper in the form of a "Legendrian knot atlas". A corresponding atlas of transverse knots can be deduced from this.

The strategy behind our atlas is a "probabilistic" approach to enumerating Legendrian and transverse knots, based on expressing them as grid diagrams. Two grid diagrams representing Legendrian or transverse knots are isotopic if and only if they are related by a sequence of elementary moves, some subset of the so-called Cromwell moves. Roughly speaking, our algorithm enumerates all grid diagrams of a particular size and attempts to determine which of them are related by these Cromwell moves. Unfortunately, one of the Cromwell moves, stabilization, changes the size of the grid

diagram, and so the algorithm cannot prove, in finite time, that two grid diagrams represent nonisotopic Legendrian or transverse knots. Nevertheless we can guess with some degree of confidence when two grids are isotopic, under the assumption that if two grid diagrams of a certain size are related by Cromwell moves, then they are related by moves that do not increase the grid size by too much.

The result of the algorithm is a computer program that can show that various grid diagrams are isotopic, and guesses that other grid diagrams are not isotopic. This technique seems to be surprisingly effective in classifying Legendrian and transverse knots. In many cases, one can prove by hand, using various recently developed invariants, that the isotopy classes of grid diagrams produced by the program are indeed distinct.

We hope that the wealth of examples produced by the atlas will be useful to researchers working in contact geometry and related fields. A precursor of sorts to this atlas, an enumeration of Legendrian representatives of knots through 9 crossings by Melvin and Shrestha [19], has provided testing material for various projects in contact topology, and many of the Melvin–Shrestha examples appear in some guise as part of our atlas.

In compiling the atlas, we discovered examples of several interesting phenomena for Legendrian and transverse knots that either had not been seen before, or had only been seen in much more complicated examples. In particular, the atlas contains:

- Legendrian (respectively transverse) knots that do not maximize Thurston–Bennequin number (self-linking number) but are not destabilizable;
- knots that can be proven to be transversely nonsimple by inspection and a bit of knot Floer homology, without computer verification or more complicated techniques;
- knots that can be proven to be transversely nonsimple only through a recently developed invariant, transverse homology, and not by knot Floer homology;
- transverse knots that are conjecturally distinct from their transverse mirrors;
- Legendrian knots with more than one linearized contact homology.

Indeed, some examples in the atlas can readily be generalized to give, for instance, infinite families of knots that can be proven to be transversely nonsimple by inspection. Furthermore, we show the following result, with an analogous statement also holding for Legendrian knots.

Proposition 1. *There are non-destabilizable prime transverse knots whose self-linking number is arbitrarily far from maximal.*

We note that similar results have been obtained by Etnyre, LaFountain, and Tosun, but with a completely different set of examples (cables of torus knots).

There are a fair number of knots in the atlas (drawn in red) that we conjecture, but are currently unable to prove, are distinct. It would be interesting to know if various "modern" techniques could be applied to these knots: Massey products on linearized contact homology [5], Legendrian Symplectic Field Theory [23], and so forth.

The atlas itself is available as a standalone file from

`http://www.math.duke.edu/~ng/atlas/`

where an analogous atlas for unoriented two-component Legendrian links, as well as various source files, can also be downloaded. Any future updates to the atlas will be posted there as well.

In Section 2, we provide a quick summary of the terms we use in the atlas, and describe the algorithm used to produce the Legendrian knot atlas. We discuss the particular examples and families of examples, illustrating the aforementioned unusual phenomena and others, in Section 3. The Legendrian knot atlas itself comprises Section 4.

Acknowledgments

The authors would like to thank John Etnyre, Hiroshi Matsuda, Dan Rutherford, Josh Sabloff, and Shea Vela-Vick for illuminating discussions. Much of this work appeared in the first author's undergraduate honors thesis at Duke University, with support from the PRUV program at Duke. The second author was supported by NSF grant DMS-0706777 and NSF CAREER grant DMS-0846346.

2. Background and Methodology

2.1. **Background.** Of the various ways to depict Legendrian and transverse knots in standard contact $\mathbb{R}^3$, we will exclusively use grid diagrams. Here we briefly recall the salient features of grid diagrams and their relationship to Legendrian and transverse knots; a more detailed discussion can be found in, e.g., [26, 28], and a more general introduction to contact knot theory in [9].

A *grid diagram* is an $n \times n$ square grid containing n X's and n O's in distinct squares, such that each row and each column contains exactly one X and one O. The *grid number* of a grid diagram is n. Given a grid diagram, one can obtain a diagram of an oriented link in $\mathbb{R}^3$ by connecting O's to X's horizontally and X's to O's vertically, and having all vertical line segments pass over all horizontal line segments wherever they cross. We will use grid diagrams and the associated link diagrams interchangeably. One can also obtain a front diagram for an oriented Legendrian link in $\mathbb{R}^3$ by rotating the link diagram 45° counterclockwise and smoothing corners. Any topological knot, and indeed any Legendrian knot, can be represented by a grid diagram; the *arc index* of a topological knot is the minimum grid number over all grid diagrams representing the knot.

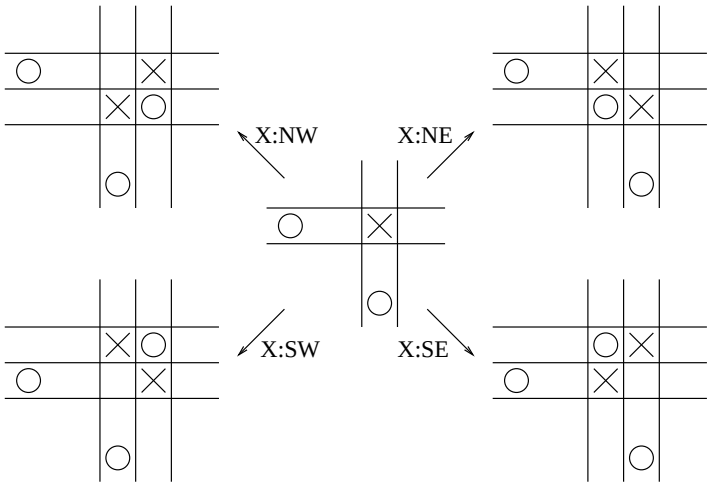

FIGURE 1. The four types of X stabilizations on a grid diagram.

There are three *Cromwell moves* relating grid diagrams, each of which preserves topological link type:

- *torus translation*, which moves the topmost row (or bottommost row, leftmost column, rightmost column) of a grid diagram to the bottommost row (topmost row, rightmost column, leftmost column) of the grid;
- *commutation*, which switches adjacent rows (columns) in which the segments connecting O's and X's are either disjoint or nested when projected to a single horizontal (vertical) line;
- *stabilization*, which increases grid number by 1 and replaces a single X (O) in the diagram by a 2×2 square with two X's (O's) and one O (X).

Of these, the most interesting to us is stabilization and its inverse operation, destabilization. Stabilization comes in eight flavors, four X stabilizations and four O stabilizations, depending on whether a single X or O is replaced and the form of the resulting 2×2 square. It suffices for our purposes to consider only the X stabilizations, which are depicted in Figure 1 (the O stabilizations are redundant).

Two grid diagrams represent isotopic topological links if and only if they are related by some sequence of Cromwell moves. We can also consider Legendrian and transverse links, up to Legendrian and transverse isotopy, to be grid diagrams modulo certain Cromwell moves:

- *Legendrian links* are grid diagrams modulo torus translation, commutation, and X:NE and X:SW stabilization and destabilization;
- *transverse links* are grid diagrams modulo torus translation, commutation, and X:NE, X:SW, and X:SE stabilization and destabilization.

In this language, an enumeration of Legendrian or transverse links up to isotopy becomes an enumeration of grid diagrams up to the appropriate equivalence relation. Also, any Legendrian link can be viewed as a transverse link; in contact topology, the resulting transverse link is called the *positive transverse pushoff* of the Legendrian link.

The *classical invariants* of Legendrian and transverse links in standard contact $\mathbb{R}^3$, which are unchanged by Legendrian or transverse isotopy, are defined in terms of a grid diagram as follows:

- the *Thurston–Bennequin number*, tb, is the writhe of the link diagram (the number of crossings counted with sign) minus the number of NE corners of the link diagram;
- the *rotation number*, r, is $1/2$ of the total number of NE and SW corners, counted with sign, where a corner is counted positively if it is traversed down and to the right, and negatively if it is traversed up and to the left;
- the *self-linking number*, sl, is $tb - r$.

The Thurston–Bennequin and rotation numbers are invariant under Legendrian isotopy, while the self-linking number is invariant under transverse isotopy.

A topological knot type is *Legendrian simple* (respectively *transversely simple*) if any two Legendrian (transverse) knots of that type with the same tb and r (sl) are necessarily Legendrian (transversely) isotopic. Any Legendrian simple knot is also transversely simple. Proofs that various knot types are Legendrian nonsimple have been obtained as applications of certain "non-classical" Legendrian invariants, such as the Legendrian contact homology of Chekanov [3] and Eliashberg and the ruling invariants of Chekanov–Pushkar [29] and Fuchs [14]. It has historically been more difficult to establish transverse nonsimplicity than Legendrian nonsimplicity.

The operations of X:NW and X:SE stabilization descend to Legendrian knots, where they become *positive* and *negative Legendrian stabilization* and change (tb, r) by $(-1, 1)$ and $(-1, -1)$, respectively. The operations of positive and negative Legendrian stabilization, which we denote by S_+ and S_-, commute up to Legendrian isotopy: $S_+S_-(L) = S_-S_+(L)$. Transverse knots can be seen as Legendrian knots modulo negative Legendrian stabilization, and the operation of X:NW stabilization descends to transverse knots, where it is called *transverse stabilization* and decreases sl by 2. If a Legendrian or transverse knot is a stabilization of another, then we say that it is *destabilizable*. Since destabilization increases tb by 1 (Legendrian) and sl by 2 (transverse), and tb and sl are bounded above in any given topological type by a classical result of Bennequin, there are non-destabilizable Legendrian and transverse knots in every knot type.

In the atlas, we depict Legendrian knots of a particular topological type via a *Legendrian mountain range*, whereby isotopy classes of Legendrian knots are plotted according to their (tb, r), with tb in the vertical direction

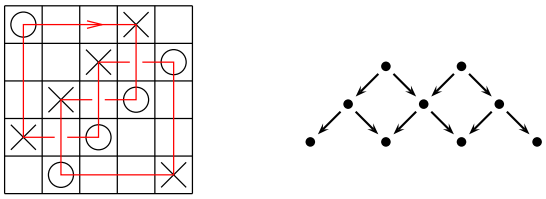

FIGURE 2. Grid diagram for a Legendrian left-handed trefoil with $(tb, r) = (-6, 1)$, and the Legendrian mountain range for the left-handed trefoil. The top row of the mountain range depicts $(tb, r) = (-6, -1)$ and $(-6, 1)$; the next row, $(tb, r) = (-7, -2)$, $(-7, 0)$, and $(-7, 2)$; and so forth. The arrows represent positive (pointing to the right) and negative (to the left) Legendrian stabilization. The mountain range continues infinitely downwards by application of stabilizations. Note that the left-handed trefoil is Legendrian simple: each value of (tb, r) has at most one Legendrian representative.

and r in the horizontal direction. Positive/negative stabilization are depicted in the mountain range by arrows pointing down and to the right/left. The classification of transverse knots of a particular topological type can be deduced from the Legendrian classification by modding out by the effect of negative Legendrian stabilization. See Figure 2.

Finally, we describe certain symmetries of Legendrian and transverse knots that are useful to consider in the atlas. Given a Legendrian knot L, one can reverse orientation to obtain the Legendrian knot $-L$; this corresponds to switching X's and O's in a grid diagram, and replaces (tb, r) by $(tb, -r)$. (Since this operation changes the underlying topological knot to its orientation reverse, it may change topological knot type in general, but all of the knots in the atlas are isotopic to their orientation reverses.) We remark that orientation reversal intertwines stabilizations: $S_+(-L) = -S_-(L)$. One can also define the *Legendrian mirror* $\mu(L)$ to be the result of applying the contactomorphism $(x, y, z) \mapsto (-x, y, -z)$ to L; this corresponds to rotating the grid diagram 180°, and replaces (tb, r) by $(tb, -r)$. The combination of the two symmetries, $L \mapsto -\mu(L)$, descends to transverse knots and is called the *transverse mirror*.

2.2. **Methodology.** Here we give a brief, and somewhat simplified, summary of the algorithm used to produce the Legendrian knot atlas. More details can be found in [4]; see `http://www.math.duke.edu/~ng/atlas/` for source files.

View the set of all grid diagrams (of arbitrary size), modulo torus translation, as an infinite graph Γ. Connect two vertices of Γ if they are related by a single commutation move, or a single stabilization move (of appropriate restricted type corresponding to Legendrian or transverse isotopy). The

connected components of Γ are precisely isotopy classes of Legendrian or transverse knots.

The graph Γ has an increasing filtration of finite subgraphs Γ_n whose vertices consist of all grid diagrams of size at most n. Determining connected components of Γ_n is a case of the familiar pathfinding problem in computer science, and approximates the problem of determining connected components of Γ.

The algorithm first produces a list of vertices of Γ_9, using a straightforward modification of the technique used by Jin, Kim, and Lee [15] to enumerate all prime knots with arc index at most 10. We eliminate grid diagrams corresponding to multicomponent links and divide the rest according to their topological knot type and classical invariants ((tb, r) for Legendrian, sl for transverse). Given the remaining grid diagrams of a particular knot type and classical invariants, the algorithm then runs a bidirectional search to determine which diagrams are connected to each other in Γ_n, where n can be adjusted and depends on the knot type, but is typically 10 or 11. This allows us to reduce the set of grid diagrams to a smaller set that is guessed by the program to represent pairwise nonisotopic Legendrian or transverse knots.

Several timesaving features have been incorporated into the actual program, which is implemented in Java, including: eliminating grid diagrams that include an adjacent X-O pair and are immediately destabilizable; first considering unoriented grid diagrams (where X's and O's are interchangeable); and adding edges corresponding to other moves that preserve Legendrian isotopy type and grid size, including the S_2 move from [26]. See [4] for details.

Because of our algorithm for constructing Legendrian knots, the completeness of our table is related to the following.

Conjecture 2. *Any Legendrian knot of maximal Thurston–Bennequin number has a grid diagram representative of minimal grid number. More generally, for a topological knot K, let $\overline{tb}(K)$ and $\alpha(K)$ denote the maximal Thurston–Bennequin number and arc index of K, respectively; then any Legendrian knot of type K and Thurston–Bennequin number $\overline{tb}(K) - m$ can be represented by a grid diagram of size $\alpha(K) + m$.*

We have expressed this statement, which is related to a question in [22], as a conjecture, although we suspect that it is probably false in general. However, it appears to be true for small knots—the program failed to find any counterexamples for small grid number—and the completeness of the atlas relies on the conjecture being true, or approximately true, for the knots in the table.

On a related note, it is interesting to find grid diagrams that are not minimal within their topological type, but nevertheless cannot be destabilized without first being stabilized; that is, non-minimal grid diagrams where torus translation and commutation (the Cromwell moves that preserve grid

number) do not suffice to produce a destabilizable diagram. The above conjecture suggests that such grid diagrams may correspond to Legendrian knots that have non-maximal tb but are non-destabilizable. It is easy to modify our program to find all such grid diagrams of a certain size. Indeed, the relevant grid diagrams of size at most 10 (which then represent knots of arc index at most 9) all produce non-maximal Legendrian knots that are either provably or conjecturally non-destabilizable. These appear in the atlas as non-maximal Legendrian knots of type $m(10_{139})$, $m(10_{145})$, 10_{161}, $m(10_{161})$, $m(12n_{242})$, and $12n_{591}$. See also the discussion in Sections 3.2 and 3.3.

3. Notable Phenomena

In this section, we observe instances of interesting behavior in the atlas. These include transverse nonsimplicity, which we extend to families beyond the knots in the atlas, and non-destabilizability for certain Legendrian knots. We also document the methods we use to distinguish various knots in the atlas.

3.1. **Transverse nonsimplicity I.** Among knots with arc index at most 9, the computer program guesses that exactly 13 are transversely nonsimple:

$$m(7_2),\ m(7_6),\ 9_{44},\ m(9_{45}),\ 9_{48},\ 10_{128},\ m(10_{132}),$$
$$10_{136},\ m(10_{140}),\ m(10_{145}),\ 10_{160},\ m(10_{161}),\ 12n_{591}.$$

These knots can be seen in the atlas as the ones whose mountain ranges (conjecturally) contain distinct Legendrian knots with the same (tb, r) that remain distinct under repeated stabilization of one type or the other. (These are pictorially represented in the atlas by mountain ranges with boxes that persist under stabilization.)

It should be emphasized that the computer program cannot prove either transverse simplicity or transverse nonsimplicity, but it can make predictions. Of the knots in the table, the program guesses that 69 are transversely simple. Of these, 18 are currently known to be transversely simple, precisely corresponding to torus knots [10] and certain twist knots [10, 13]:

$$3_1,\ m(3_1),\ 4_1,\ 5_1,\ m(5_1),\ 5_2,\ m(5_2),\ 6_1,\ m(6_1),\ 7_1,\ m(7_1),\ 7_2,$$
$$8_{19},\ m(8_{19}),\ 10_{124},\ m(10_{124}),\ 15n_{41185},\ m(15n_{41185}).$$

Proving transverse simplicity for the remaining 51 knots appears to be difficult and might involve convex surface techniques as in [10, 13].

On the other hand, proving transverse nonsimplicity can sometimes be a simple matter of applying one of the known transverse invariants.[1] The $\widehat{\theta}$ transverse invariant in knot Floer homology of Ozsváth, Szabó, and Thurston [28] proves that 5 of the 13 transversely nonsimple candidates listed above

[1]The techniques of Birman and Menasco [1, 2] are another approach to transverse nonsimplicity, but the knots of braid index 3 that they have proven to be transversely nonsimple all have arc index at least 10 and are not covered in the atlas.

are indeed transversely nonsimple: $m(10_{132})$, $m(10_{140})$, $m(10_{145})$, $m(10_{161})$, and $12n_{591}$. In each of these cases, the computer program of [25] demonstrates that $\widehat{\theta}$ is zero for one of the transverse representatives and nonzero for the other. (In particular, this precise computation is presented in [25] for $m(10_{132})$ and $m(10_{140})$.) A related transverse invariant in knot Floer homology due to [17] has been used in [27] to prove transverse nonsimplicity for $m(7_2)$.

Recently a new transverse invariant, transverse homology, has been introduced by the second author in collaboration with Ekholm, Etnyre, and Sullivan; see [7, 24]. As described in [24], transverse homology proves transverse nonsimplicity for 10 of the above 13 candidates, including the 5 also given by knot Floer homology: $m(7_2)$, $m(7_6)$, 9_{44}, 9_{48}, $m(10_{132})$, 10_{136}, $m(10_{140})$, $m(10_{145})$, $m(10_{161})$, $12n_{591}$.

In all cases involving transverse nonsimplicity, the precise statement is as follows: for a particular knot type, there are two grid diagrams in the atlas representing Legendrian knots L_1, L_2 of that knot type, such that the positive transverse pushoffs of L_1, L_2 are not transversely isotopic. It follows that arbitrary negative Legendrian stabilizations of L_1, L_2 are distinct, as are arbitrary positive Legendrian stabilizations of $-L_1, -L_2$ (alternatively, positive Legendrian stabilizations of $\mu(L_1), \mu(L_2)$). For an enumeration of which specific grid diagrams in the atlas correspond to distinct transverse knots, see Table 2 at the end of the atlas.

There are 4 instances where the atlas guesses, but the above invariants so far fail to prove, that certain transverse knots are distinct. These are the 3 knots $m(9_{45})$, 10_{128}, and 10_{160}, which we conjecture but cannot prove are transversely nonsimple, and the knot 9_{44}, where the program finds three possibly distinct transverse knots but the invariants can only distinguish two. In all these cases, the issue is a subtle involutive operation on transverse knots called the transverse mirror [26]. In terms of Legendrian knots, this operation can be described as follows: given a Legendrian knot L, the positive transverse pushoffs of L and $-\mu(L)$ are defined to be transverse mirrors. (In general, transverse mirrors are topologically related by orientation reversal, but all of the topological knots in the atlas are invariant under orientation reversal.) Transverse mirrors are difficult to distinguish using the known invariants, and the transverse mirror pairs in the 4 knot types above are conjectured but not proven to be distinct.

3.2. **Transverse nonsimplicity II.** Three of the transversely nonsimple knot types described in the previous section—$m(10_{145})$, $m(10_{161})$, and $12n_{591}$—merit further discussion. These are knots with a transverse representative that does not maximize self-linking number but is non-destabilizable.

Proposition 3. *In each of the knot types $m(10_{145})$, $m(10_{161})$, and $12n_{591}$, there are transverse knots T_1, T_2 for which $sl(T_2) = sl(T_1) - 2$ but T_2 is not the stabilization of any transverse knot.*

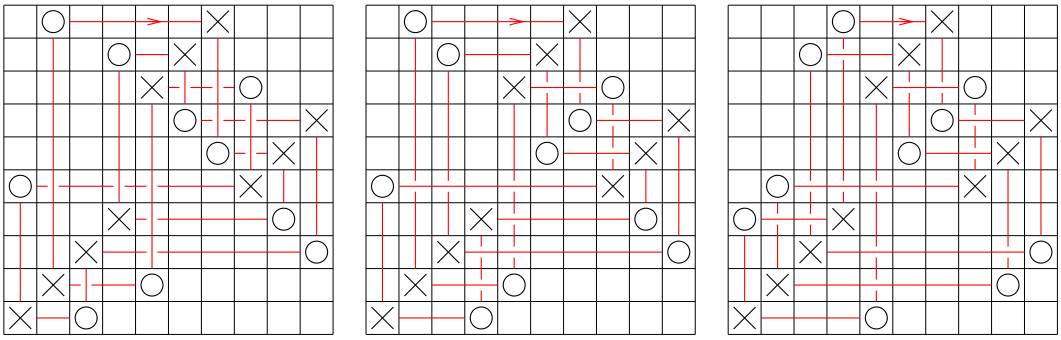

FIGURE 3. Grid diagrams representing nondestabilizable transverse knots of type $m(10_{145})$, $m(10_{161})$, and $12n_{591}$.

Proof. This result can be proven using either of the transverse invariants discussed in the previous section, but it is easiest to use the $\widehat{\theta}$ invariant in knot Floer homology. Consider the grid diagrams shown in Figure 3.[2] In each case, the positive transverse pushoff T_2 of the grid diagram does not maximize self-linking number, as can be seen by inspection of the atlas. However, it can also be seen by inspection that $\widehat{\theta}$ is nonzero for each of the diagrams: $\widehat{\theta}$ is represented in the Manolescu–Ozsváth–Sarkar complex for $\widehat{HFK}$ by the upper-right corners of the X's, and it is clear in each case that this generator is not in the image of the differential, since there are no empty rectangles with NW-SE corners at two of these upper-right corners. By a result of [28], $\widehat{\theta} = 0$ for stabilizations of transverse knots; it follows that T_2 is not a stabilization in each case. □

Two remarks are in order. First, the phenomenon of knots with a non-maximal, non-destabilizable transverse representative was first demonstrated by Etnyre and Honda [11], who showed that the $(2,3)$ cable of the $(2,3)$ torus knot has this property; there is also recent work by Lafontaine and Tosun, as well as Matsuda, in this regard. However, the examples in Proposition 3 are significantly simpler in various ways than cables of torus knots. For example, Shonkwiler and Vela-Vick [30] have shown that the Legendrian contact homology of the $m(10_{161})$ knot in Proposition 3 is nontrivial, while an analagous statement for the $(2,3)$ cable of the $(2,3)$ torus knot is still open.

[2]A note on conventions: to obtain grid diagrams as in Figure 3 for which we can apply $\widehat{\theta}$ as in [28], we either rotate a usual X-O diagram 90° counterclockwise and interchange X's and O's (for the third diagram in Figure 3), or rotate a usual X-O diagram 90° clockwise (for the first two diagrams). In the resulting diagrams, we use the convention from [28] that horizontal segments pass *over* vertical segments. The resulting Legendrian front is either identical to the original front (for the third diagram), or related to the original front by the transformation $L \mapsto -\mu(L)$ (for the first two diagrams; for both, the atlas states that this transformation is a Legendrian isotopy), possibly along with a few elementary moves in Gridlink [6].

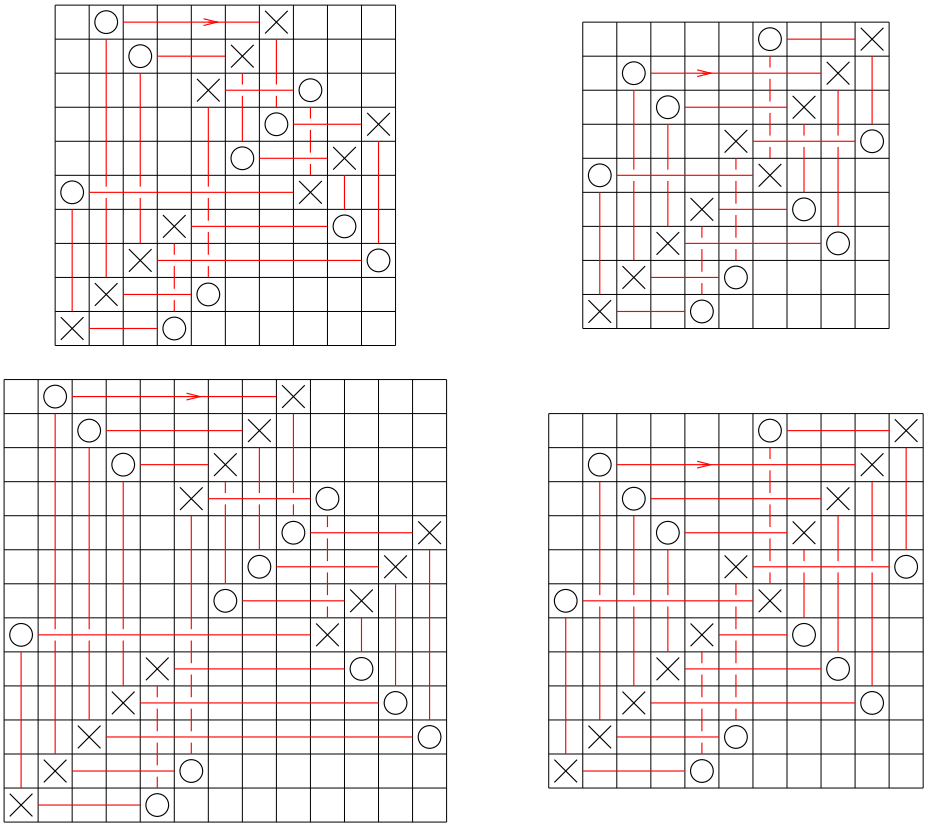

FIGURE 4. Grid diagrams for nondestabilizable transverse knots $T_{n,2}$ (left) and topologically isotopic transverse knots $T_{n,1}$ (right), for $n = 1, 2$.

Second, Proposition 3 is an application of the transverse HFK invariant that involves no computation, only an inspection of a grid diagram. Previous applications of $\widehat{\theta}$ to transverse nonsimplicity involved a computer program ([25]), an examination of naturality ([27]), or some relatively intricate linear algebra ([16]). The simplicity of the proof of Proposition 3 suggests that the knots considered there might be easily generalized to infinite families of interesting nondestabilizable transverse knots. This is indeed the case.

Proposition 4. *For any $n \geq 1$, there is a topological knot K_n with two transverse representatives $T_{n,1}, T_{n,2}$ such that*

$$sl(T_{n,2}) = sl(T_{n,1}) - 2n$$

but $T_{n,2}$ is not the stabilization of any transverse knot. In particular, K_n is transversely nonsimple.

Proposition 4 as stated is already known and follows from work of Etnyre and Honda [12]: given K_1, one can use the n-th connected sum of K_1 with

itself as K_n. However, the family K_n we present in the proof of Proposition 4 consists of prime knots. We will only sketch a proof of primality and segregate this result as Proposition 5 below.

It should be noted that Hiroshi Matsuda has independently obtained results similar to Proposition 4 (indeed, with apparently the same family of examples); see the proof of Proposition 5.

Proof of Proposition 4. The grid diagram for $m(10_{161})$ given in Figure 3 generalizes readily to a family of grid diagrams of size $3n+7$ and self-linking number $2n+1$, as shown (for $n=1,2$) on the left hand side of Figure 4; call the positive transverse pushoff of these diagrams $T_{n,2}$. By inspection, $\widehat{\theta}(T_{n,2}) \neq 0$ since there are no empty rectangles with NW-SE corners at upper right corners of X's. On the other hand, $T_{n,2}$ is evidently topologically isotopic to the grid diagram on the right hand side of Figure 4, whose positive transverse pushoff is a transverse knot $T_{n,1}$ with self-linking number $4n+1$. □

Proposition 5. *The family of knots K_n in Proposition 4 can be chosen to be prime.*

Outline of proof. It is straightforward to check from Figure 4 that $T_{n,2}$ is topologically the closure of the braid

$$(\sigma_1\sigma_2\cdots\sigma_{n+2})\sigma_{n+2}\sigma_{n+1}^{-3}\sigma_n\cdots\sigma_2\sigma_1(\sigma_1\sigma_2\cdots\sigma_{n+2})\sigma_n\cdots\sigma_2\sigma_1(\sigma_1\sigma_2\cdots\sigma_{n+2})\in B_{n+3};$$

the diagram for $T_{n,2}$ is essentially braided clockwise around the middle of the grid. We claim that topological type K_n of $T_{n,2}$ is prime. The braid above is related by an operation discovered by Matsuda called an "H-flype", which preserves topological knot type of the braid closure, to the braid

$$(\sigma_1\sigma_2)\sigma_2(\sigma_1\sigma_2)\sigma_2^{-3}((\sigma_1\sigma_2)(\sigma_2\sigma_1))^n(\sigma_1\sigma_2)=\sigma_2^{-2}\sigma_1(\sigma_2^2\sigma_1^2)^{n+1}\sigma_2\in B_3.$$

To show that the closure of a 3-braid is prime, it suffices to check that it is not a $(2,k)$ torus knot or the connected sum of two such torus knots. In this case, this can be shown by calculating the Alexander and Jones polynomials of the closure of $\sigma_2^{-2}\sigma_1(\sigma_2^2\sigma_1^2)^{n+1}\sigma_2$ and comparing to the Alexander and Jones polynomials of $(2,k)$ torus knots. □

3.3. **Non-maximal, non-destabilizable Legendrian knots.** Each of the examples from the preceding section (non-destabilizable transverse knots with non-maximal self-linking number) produces an analogous phenomenon for Legendrian knots: a non-destabilizable Legendrian knot with non-maximal Thurston–Bennequin number.

Proposition 6. *In each of the knot types $m(10_{145})$, $m(10_{161})$, and $12n_{591}$, there are Legendrian knots L_1, L_2, L_3 for which $tb(L_1) = tb(L_2)+1 = tb(L_3)+2$ but neither L_2 nor L_3 is not the stabilization of any Legendrian knot.*

Proof. We prove the result for $m(10_{145})$; the proof for the other two knots is nearly identical. Let L_1, L_2, L_3 be the Legendrian $m(10_{145})$ knots in the atlas with $(tb, r) = (3,0), (2,1), (1,0)$, respectively; note that L_2 is isotopic to the leftmost diagram in Figure 3. Since the positive transverse pushoff of L_2 is non-destabilizable by Proposition 3, L_2 is not the negative stabilization of any Legendrian knot. On the other hand, the HOMFLY-PT polynomial bound of Morton and Franks–Williams states for all Legendrian $m(10_{145})$ knots L that $tb(L) + |r(L)| \leq 3$. In particular, there is no L with $(tb, r) = (3,2)$, and thus L_2 is not the positive stabilization of any Legendrian knot.

The computer program of [25] shows that L_3 and $-L_3$ both have nonzero $\widehat{\theta}$ invariant; in the language of [25, 28], both $\lambda_+(L_3)$ and $\lambda_-(L_3)$ are nonzero in homology. Thus neither L_3 nor $-L_3$ is negatively destabilizable, and it follows that L_3 is neither positively nor negatively destabilizable. □

Shonkwiler and Vela-Vick [30] have provided an alternate proof that the knot L_2 for $m(10_{161})$ in Proposition 6 is non-destabilizable, using Legendrian contact homology and the characteristic algebra.

One can extend the argument of Proposition 4 to prove the existence for any $n \geq 1$ of a prime knot K_n with Legendrian representatives $L_{n,1}, L_{n,2}$ for which $tb(L_{n,2}) = tb(L_{n,1}) - 2n$ but $L_{n,2}$ is not destabilizable. We remark that B. Tosun has obtained a similar result by studying cables of torus knots.

We can use the preceding discussion to examine the Legendrian mountain range for $m(10_{145})$, with similar analysis for $m(10_{161})$ and $12n_{591}$. The shape of the mountain range shown in the atlas is determined by Proposition 3, along with the following result.

Proposition 7. *There are at least four distinct $m(10_{145})$ knots with $(tb, r) = (1,0)$. (Note that $\overline{tb}(m(10_{145})) = 3$.)*

Proof. Let L_1, L_2, L_3 be the Legendrian $m(10_{145})$ knots from (the proof of) Proposition 6. We claim that $S_+S_-(L_1)$, $S_-(L_2)$, $S_+(-L_2)$, and L_3 are pairwise distinct.

Since L_3 is non-destabilizable by the proof of Proposition 6, it is distinct from $S_+S_-(L_1)$, $S_-(L_2)$, and $S_+(-L_2)$. Since L_2 and $S_+(L_1)$ have nonisotopic positive transverse pushoffs, $S_-(L_2)$ and $S_-S_+(L_1) = S_+S_-(L_1)$ are distinct, as are $S_+(-L_2) = -S_-(L_2)$ and $S_+S_-(L_1) = -S_+S_-(L_1)$.

It remains to show that $S_-(L_2)$ and $S_+(-L_2)$ are distinct. One can verify by computer that $S_-^2(L_1) = S_-(-L_2)$, and so $S_+S_-(-L_2) = S_+S_-^2(L_1)$. On the other hand, since L_2 and $S_+(L_1)$ have distinct positive transverse pushoffs, $S_-^2(L_2) \neq S_+S_-^2(L_1) = S_+S_-(-L_2)$. Thus $S_-(L_2) \neq S_+(-L_2)$, as desired. □

It is interesting to compare the mountain ranges of $m(10_{145})$, $m(10_{161})$, and $12n_{591}$ with the mountain range of the $(2,3)$ cable of the $(2,3)$ torus knot from [11], which exhibits similar behavior but is slightly different.

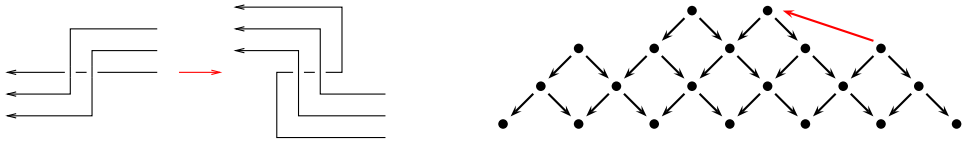

FIGURE 5. A local move on Legendrian knots, preserving topological type and changing (tb, r) by $(+1, -3)$. On the right, the move in the context of the mountain range for $m(10_{139})$, 10_{161}, or $m(12n_{242})$.

Besides $m(10_{145})$, $m(10_{161})$, and $12n_{591}$, the atlas produces three other candidates for knots with non-maximal non-destabilizable Legendrian representatives: $m(10_{139})$, 10_{161}, and $m(12n_{242})$. For these knots, it appears that a new behavior emerges: the mountain ranges seem to have non-maximal peaks.

Conjecture 8. *For each of $m(10_{139})$, 10_{161}, and $m(12n_{242})$, there exists a Legendrian knot L with $tb(L)$ strictly less than the maximal possible tb, for which there is no other Legendrian representative with $(tb, r) = (tb(L) + 1, r(L) + 1)$ or $(tb(L) + 1, r(L) - 1)$.*

It may be worth remarking that the transverse techniques from the previous sections are not applicable to Conjecture 8; it appears that there is a unique non-destabilizable transverse knot in each of the knot types. In addition, contact homology fails to provide an obstruction to destabilizability: the non-maximal, conjecturally non-destabilizable Legendrian knots of type $m(10_{139})$, 10_{161}, and $m(12n_{242})$ in the atlas all have vanishing Legendrian contact homology.

As a side note, each of the three knots in Conjecture 8 has a "local move" relating a non-maximal peak to a maximal peak, shown in Figure 5. Presumably this move can be used to construct many more examples of knots with non-maximal peaks in their mountain ranges.

3.4. **Multiple linearized contact homologies.** Melvin and Shrestha [19] discovered the phenomenon of Legendrian knots that have more than one possible linearized contact homology (corresponding to different augmentations of the Chekanov–Eliashberg differential graded algebra). Their examples included the knots listed in our atlas as $m(8_{21})$ and (the second representative of) $m(9_{45})$.

Our atlas provides more examples of Legendrian knots with multiple linearized contact homologies, of topological type $11n_{95}$ and $11n_{118}$. In addition, the atlas finds another $m(9_{45})$ example with multiple linearized contact homologies, distinct from the Melvin–Shrestha example.

3.5. **Discussion of other particular knots.** In the atlas, there are many instances of Legendrian knots with the same classical invariants (topological type, Thurston–Bennequin number, and rotation number) that are provably

or conjecturally non-isotopic. Often these can be distinguished from each other by (0-)graded ruling invariant or linearized contact homology, both included in the atlas. The computations for ruling invariant and linearized contact homology were performed using [18].

Transverse nonsimplicity, as discussed in Sections 3.1 and 3.2, distinguishes other Legendrian knots. For transversely nonsimple knots, there is a diagonal of nonisotopic Legendrian knots with the same classical invariants that travels down and to the left (following negative Legendrian stabilization), and another diagonal down and to the right (following positive stabilization).

Here we document the remaining cases of Legendrian knots in the atlas that we can provably distinguish by other means. We use the convention that in a particular knot type, the grid diagrams depicted in the atlas represent Legendrian knots labeled $L_1, L_2, L_3, \ldots$ from top to bottom.

- 6_2: The fact that the listed knot with $(tb, r) = (-7, 0)$ is not Legendrian isotopic to its mirror is proven in [20], with a reproof in [21].
- 6_3: The two Legendrian 6_3 knots in the table have previously been considered in [21, section 4.3], where they are called K_4 and K_3, respectively, and are proven to be distinct via the characteristic algebra.
- $m(7_2)$: The fact that there are five distinct Legendrian representatives with $(tb, r) = (1, 0)$, including a pair of nonisotopic mirrors, is proven in [13] and essentially follows from the work on transverse twist knots in [27].
- 7_4: Linearized contact homology distinguishes L_4 from the other three. The knots L_2, L_3 were considered in [21, section 4.2], where they were called K_1, K_2, respectively. As noted in [21], these two knots can be distinguished by their characteristic algebras. A minor extension of the argument from [21] also shows that $L_3 = K_2$ is not Legendrian isotopic to its Legendrian mirror: in the characteristic algebra for K_2, there are elements a_{13} and a_{12} with degrees -2 and 2, respectively, for which $a_{13}a_{12} = 1$, but no elements x, y with degrees 2 and -2, respectively, for which $xy = 1$. See also [21, section 4.1]. Since the computer program shows that L_1 and L_2 are each isotopic to their mirrors, neither is isotopic to L_3. It is an interesting open problem to distinguish L_1 and L_2.
- $m(7_6)$: Linearized contact homology distinguishes L_3 and $-L_3$ from L_1 and L_2. The computer program shows that $L_1, -L_3$ have the same negative stabilization, as do $L_2, -L_2, L_3$; see Table 2. On the other hand, from [24], L_1 and L_2 represent distinct transverse knots. Thus $L_1, -L_3$ are distinct from $L_2, -L_2, L_3$ as Legendrian knots. Since $L_1 = -L_1$ by the computer program, orientation reversal implies that L_1, L_3 are distinct from $L_2, -L_2, -L_3$. As a result,

$L_1, L_3, -L_3$ are pairwise distinct, and all are distinct from $L_2, -L_2$. We do not currently know if L_2 and $-L_2$ are isotopic.

- 9_{48}, $m(10_{132})$, 10_{136}, $m(10_{140})$: The Legendrian knots of these types are distinguished using the data from Table 2, in a manner similar to $m(7_6)$ above.

4. The Legendrian Knot Atlas

The table on the following pages depicts conjectural classifications of Legendrian knots in all prime knot types of arc index up to 9. For each knot, we present a conjecturally complete list of non-destabilizable Legendrian representatives, modulo the symmetries of orientation reversal $L \mapsto -L$ and Legendrian mirroring $L \mapsto \mu(L)$. As usual, rotate 45° counterclockwise to translate from grid diagrams to fronts.

Each knot also comes with its conjectural Legendrian mountain range (extending infinitely downwards), comprised of black and red dots, plotted according to their Thurston–Bennequin number (vertical) and rotation number (horizontal). Arrows represent positive and negative Legendrian stabilization. The values of (tb, r) are not labeled but can be deduced from the values given for the non-destabilizable representatives. Boxes surround values of (tb, r) that have, or appear to have, more than one Legendrian representative, and mountain ranges without boxes represent knot types that are conjecturally Legendrian simple. The dots represent conjecturally distinct Legendrian isotopy classes; black dots are provably distinct classes, while red dots are conjecturally but not provably distinct from the black dots and each other. Thus the black dots represent a lower bound for the Legendrian mountain range, and the totality of dots represent our current best guess for the precise mountain range (which however could theoretically be larger or smaller than what is depicted).

Legendrian knots have been classified for several knot types, including torus knots and 4_1 [10] and twist knots [13]. These comprise the knots $3_1, 4_1, 5_1, 5_2, 6_1, 7_1, 7_2$ in the table, along with their mirrors; for these knots, the mountain ranges depicted in the atlas agree with the classification results. In the table, we indicate torus knots by $T(p, q)$ and twist knots by K_n (for the knot with n half-twists, with the convention of [13]).

Using symmetries, we can produce from any Legendrian knot L up to four possibly distinct Legendrian knots: L, $-L$, $\mu(L)$, and $-\mu(L)$. The table depicts one representative from each of these orbits of up to four knots, along with information about which of the four knots in the orbit are isotopic, if any. For knots with nonzero rotation number, we choose a representative L with positive rotation number, and L is trivially distinct from $-L$ and $\mu(L)$ (this fact depicted by hyphens in the table).

Grid diagrams labeled with matching letters (see e.g. 6_2) mark Legendrian knots that we believe but cannot yet prove to be distinct. Question marks indicate knots where we believe but cannot prove that L is distinct from

$-L$, $\mu(L)$, or $-\mu(L)$. All check marks have been verified by computer. All X marks without question marks have been proven, via various techniques. These techniques include two nonclassical Legendrian invariants, the graded ruling invariant [29] and the set of (Poincaré polynomials for) linearized contact homologies [3], which have been computed, where relevant, using the *Mathematica* notebook [18]. (Knots with no graded rulings/augmentations are denoted in these columns by a hyphen, for nonzero rotation number, or $\emptyset$, for zero rotation number.) For Legendrian knots that we have succeeded in distinguishing by means besides these invariants, please see Section 3 for documentation.

For some knots, the atlas omits a bit of information necessary to deduce a complete (conjectural) Legendrian classification, namely which Legendrian knots with the same (tb, r) stabilize to isotopic knots. This information is presented in Table 2, which follows the atlas. The knots given in Table 2 are those where there is some ambiguity about isotopy classes after stabilization; for all of those knots, the program guesses that the relevant Legendrian representatives either become isotopic after one (positive or negative) stabilization, or remain nonisotopic after arbitrarily many stabilizations.

TABLE 1. Atlas of Legendrian Knots up to arc index 9

Knot Type	Grid Diagram	(tb, r)	$L = -L$?	$L = \mu(L)$?	$L = -\mu(L)$?	Ruling Invariant	Linearized Contact Homology	Note
3_1	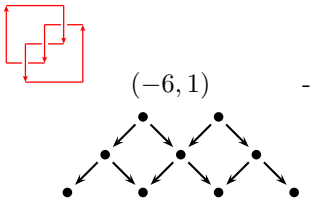	$(-6, 1)$	-	-	✓	-	-	$T(2,-3)$, K_1
$m(3_1)$	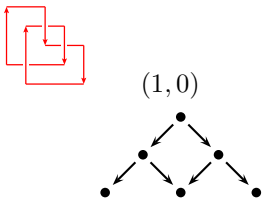	$(1, 0)$	✓	✓	✓	$2 + z^2$	$2 + t$	$T(2,3)$, K_{-2}
$4_1 = m(4_1)$	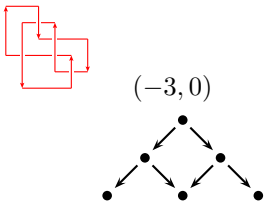	$(-3, 0)$	✓	✓	✓	1	$t^{-1} + 2t$	$K_2 = K_{-3}$
5_1	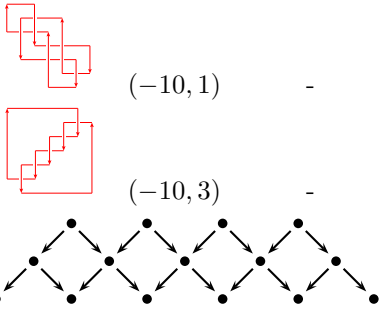	$(-10, 1)$ $(-10, 3)$	- -	- -	✓ ✓	- -	- -	$T(2,-5)$

Knot Type	Grid Diagram	(tb, r)	$L = -L$?	$L = \mu(L)$?	$L = -\mu(L)$?	Ruling Invariant	Linearized Contact Homology	Note
$m(5_1)$	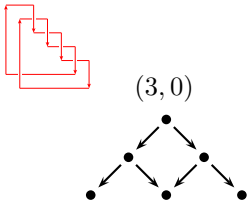	$(3, 0)$	✓	✓	✓	$3 + 4z^2 + z^4$	$4 + t$	$T(2, 5)$
5_2	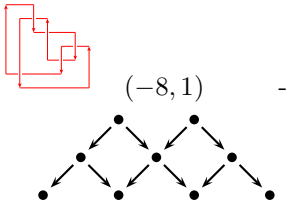	$(-8, 1)$	-	-	✓	-	-	K_3
$m(5_2)$	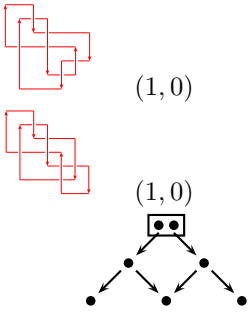	$(1, 0)$	✓	✓	✓	1	$t^{-2} + t + t^2$	K_{-4}
		$(1, 0)$	✓	✓	✓	$1 + z^2$	$2 + t$	
6_1	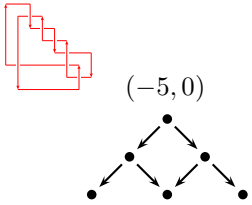	$(-5, 0)$	✓	✓	✓	1	$2t^{-1} + 3t$	K_4

†

Knot Type	Grid Diagram	(tb, r)	$L = -L$?	$L = \mu(L)$?	$L = -\mu(L)$?	Ruling Invariant	Linearized Contact Homology	Note
$m(6_1)$	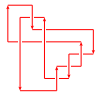	$(-3, 0)$	✓	✓	✓	1	$t^{-3} + t + t^3$	K_{-5}
	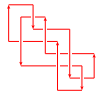	$(-3, 0)$	✓	✓	✓	1	$t^{-1} + 2t$	
	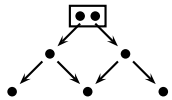							
6_2	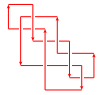	$(-7, 0)$	✓	✗	✗	$\emptyset$	$\emptyset$	
	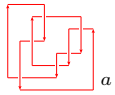	$(-7, 2)$	-	-	✓	-	-	
		$(-7, 2)$	-	-	✓	-	-	
	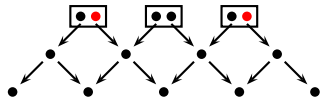							
$m(6_2)$	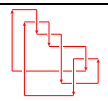	$(-1, 0)$	✓	✓	✓	$2 + z^2$	$t^{-1} + 2 + 2t$	
	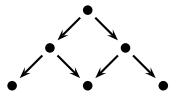							

Knot Type	Grid Diagram	(tb, r)	$L = -L$?	$L = \mu(L)$?	$L = -\mu(L)$?	Ruling Invariant	Linearized Contact Homology	Note
$6_3 = m(6_3)$	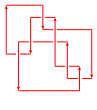	$(-4, 1)$	-	-	✓	-	-	
		$(-4, 1)$	-	-	✓	-	-	
	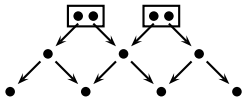							
7_1		$(-14, 1)$	-	-	✓	-	-	$T(2, -7)$
		$(-14, 3)$	-	-	✓	-	-	
		$(-14, 5)$	-	-	✓	-	-	
	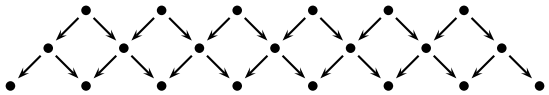							
$m(7_1)$	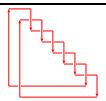	$(5, 0)$	✓	✓	✓	$4 + 10z^2 + 6z^4 + z^6$	$6 + t$	$T(2, 7)$
	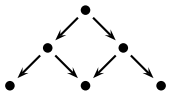							

Knot Type	Grid Diagram	(tb, r)	$L = -L$?	$L = \mu(L)$?	$L = -\mu(L)$?	Ruling Invariant	Linearized Contact Homology	Note
7_2	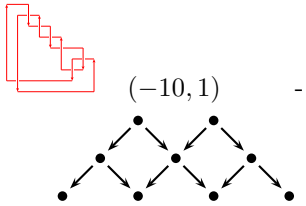	$(-10, 1)$	-	-	✓	-	-	K_5
$m(7_2)$	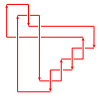	$(1, 0)$	✓	✓	✓	1	$t^{-4} + t + t^4$	K_{-6}
	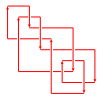	$(1, 0)$	✓	✓	✓	$1 + z^2$	$2 + t$	
		$(1, 0)$	✗	✗	✓	1	$t^{-2} + t + t^2$	
		$(1, 0)$	✓	✓	✓	$1 + z^2$	$2 + t$	
	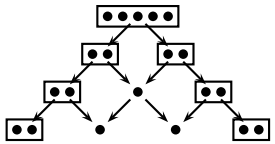							
7_3	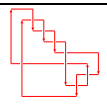	$(3, 0)$	✓	✓	✓	1	$2t^{-2} + t + 2t^2$	
		$(3, 0)$	✓	✓	✓	$1 + 3z^2 + z^4$	$4 + t$	
	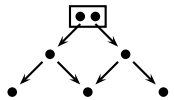							

Knot Type	Grid Diagram	(tb, r)	$L = -L$?	$L = \mu(L)$?	$L = -\mu(L)$?	Ruling Invariant	Linearized Contact Homology	Note
$m(7_3)$	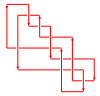	$(-12, 1)$	-	-	✓	-	-	
	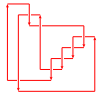	$(-12, 3)$	-	-	✓	-	-	
	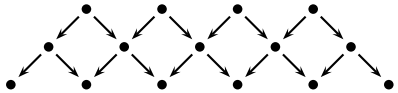							
7_4		$(1, 0)$	✓	✓	✓	$\emptyset$	$\emptyset$	
	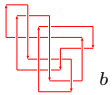	$(1, 0)$	✓	✓	✓	$\emptyset$	$\emptyset$	
		$(1, 0)$	✓	✗	✗	$\emptyset$	$\emptyset$	
		$(1, 0)$	✓	✓	✓	z^2	$2 + t$	
	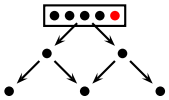							
$m(7_4)$	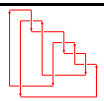	$(-10, 1)$	-	-	✓	-	-	
	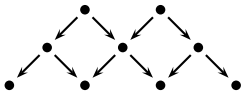							

Knot Type	Grid Diagram	(tb, r)	$L = -L$?	$L = \mu(L)$?	$L = -\mu(L)$?	Ruling Invariant	Linearized Contact Homology	Note
7_5	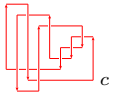	$(-12, 1)$	-	-	✓	-	-	
	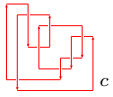	$(-12, 1)$	-	-	✓	-	-	
	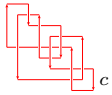	$(-12, 1)$	-	-	✓	-	-	
	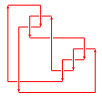	$(-12, 3)$	-	-	✓	-	-	
	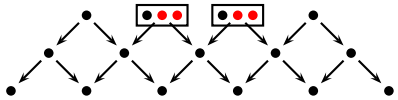							
$m(7_5)$	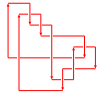	$(3, 0)$	✓	✓	✓	$2 + z^2$	$t^{-2} + 2 + t + t^2$	
	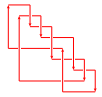	$(3, 0)$	✓	✓	✓	$2 + 3z^2 + z^4$	$4 + t$	
	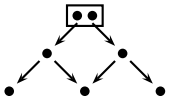							

Knot Type	Grid Diagram	(tb, r)	$L = -L$?	$L = \mu(L)$?	$L = -\mu(L)$?	Ruling Invariant	Linearized Contact Homology	Note
7_6	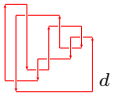	$(-8, 1)$	-	-	✓	-	-	
		$(-8, 1)$	-	-	✓	-	-	
	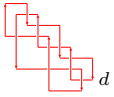	$(-8, 1)$	-	-	✗?	-	-	
$m(7_6)$		$(-1, 0)$	✓	✓	✓	$1 + z^2$	$t^{-1} + 2 + 2t$	
		$(-1, 0)$	✗?	✗?	✓	$1 + z^2$	$t^{-1} + 2 + 2t$	
		$(-1, 0)$	✗	✗	✓	1	$t^{-2} + t^{-1} + 2t + t^2$	

Knot Type	Grid Diagram	(tb, r)	$L = -L$?	$L = \mu(L)$?	$L = -\mu(L)$?	Ruling Invariant	Linearized Contact Homology	Note
7_7	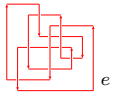	$(-4, 1)$	-	-	✗?	-	-	
		$(-4, 1)$	-	-	✓	-	-	
	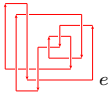	$(-4, 1)$	-	-	✓	-	-	
	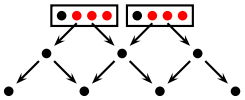							
$m(7_7)$	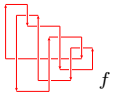	$(-5, 0)$	✓	✓	✓	1	$2t^{-1} + 3t$	
		$(-5, 0)$	✓	✓	✓	1	$2t^{-1} + 3t$	
	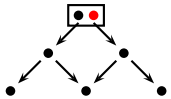							
8_{19}		$(5, 0)$	✓	✓	✓	$5 + 10z^2 + 6z^4 + z^6$	$6 + t$	$T(3, 4)$
	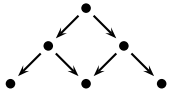							

Knot Type	Grid Diagram	(tb, r)	$L = -L$?	$L = \mu(L)$?	$L = -\mu(L)$?	Ruling Invariant	Linearized Contact Homology	Note
$m(8_{19})$	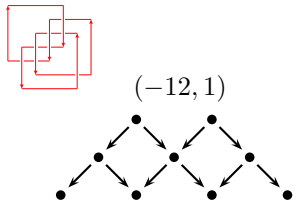	$(-12, 1)$	-	-	✓	-	-	$T(3,-4)$
8_{20}	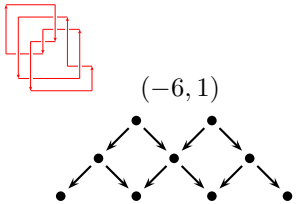	$(-6, 1)$	-	-	✓	-	-	
$m(8_{20})$	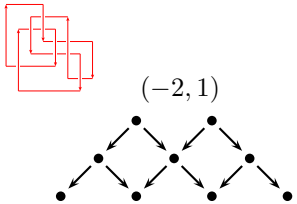	$(-2, 1)$	-	-	✓	-	-	
8_{21}	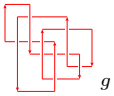 g	$(-9, 0)$	✓	✓	✓	$\emptyset$	$\emptyset$	
	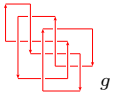 g	$(-9, 0)$	✓	✗?	✗?	$\emptyset$	$\emptyset$	
	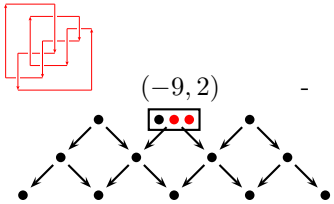	$(-9, 2)$	-	-	✓	-	-	

Knot Type	Grid Diagram	(tb, r)	$L = -L$?	$L = \mu(L)$?	$L = -\mu(L)$?	Ruling Invariant	Linearized Contact Homology	Note
$m(8_{21})$	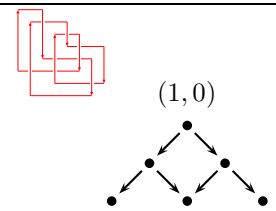	$(1, 0)$	✓	✓	✓	$3 + 2z^2$	$2 + t$, $t^{-1} + 4 + 2t$	
9_{42}	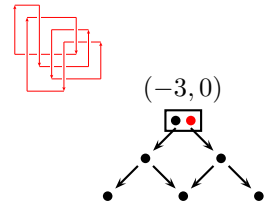	$(-3, 0)$	✓	✗?	✗?	$2 + z^2$	$2t^{-1} + 2 + 3t$	
$m(9_{42})$	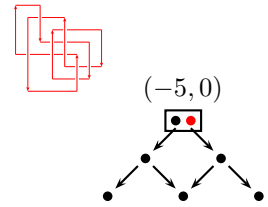	$(-5, 0)$	✗?	✗?	✓	$\emptyset$	$\emptyset$	
9_{43}	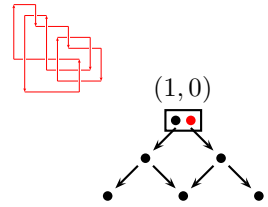	$(1, 0)$	✗?	✗?	✓	$3 + 4z^2 + z^4$	$t^{-1} + 4 + 2t$	
$m(9_{43})$	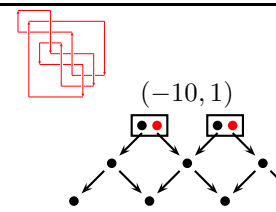	$(-10, 1)$	-	-	✗?	-	-	

Knot Type	Grid Diagram	(tb, r)	$L = -L$?	$L = \mu(L)$?	$L = -\mu(L)$?	Ruling Invariant	Linearized Contact Homology	Note
9_{44}		$(-6, 1)$	-	-	✗?	-	-	
		$(-6, 1)$	-	-	✗?	-	-	
	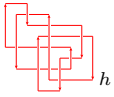	$(-6, 1)$	-	-	✗?	-	-	
$m(9_{44})$		$(-3, 0)$	✗?	✓	✗?	1	$t^{-1} + 2t$	
9_{45}		$(-10, 1)$	-	-	✗?	-	-	
	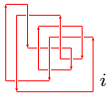	$(-10, 1)$	-	-	✓	-	-	
	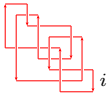	$(-10, 1)$	-	-	✗?	-	-	

Knot Type	Grid Diagram	(tb, r)	$L = -L$?	$L = \mu(L)$?	$L = -\mu(L)$?	Ruling Invariant	Linearized Contact Homology	Note
$m(9_{45})$	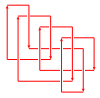	$(1,0)$	✗?	✗?	✗?	$2+2z^2$	$2+t,\ t^{-1}+4+2t$	
	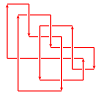	$(1,0)$	✓	✗?	✗?	$2+z^2$	$2+t,\ t^{-2}+t^{-1}+2+2t+t^2$	
	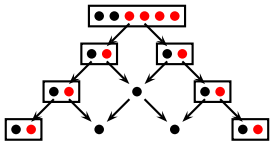							
9_{46}	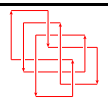	$(-7,0)$	✓	✓	✓	1	$3t^{-1}+4t$	
	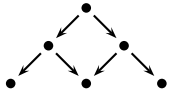							
$m(9_{46})$	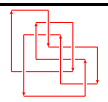	$(-1,0)$	✓	✓	✓	2	t	
	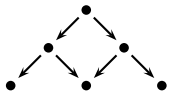							
9_{47}	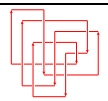	$(-2,1)$	-	-	✓	-	-	
	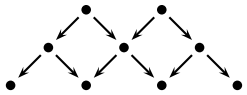							

Knot Type	Grid Diagram	(tb, r)	$L = -L$?	$L = \mu(L)$?	$L = -\mu(L)$?	Ruling Invariant	Linearized Contact Homology	Note
$m(9_{47})$		$(-7, 0)$ 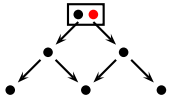	✗?	✗?	✓	1	$3t^{-1} + 4t$	
9_{48}	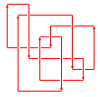	$(-1, 0)$	✓	✓	✓	z^2	$t^{-1} + 2 + 2t$	
	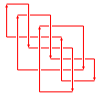	$(-1, 0)$	✗?	✗?	✓	z^2	$t^{-1} + 2 + 2t$	
	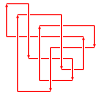	$(-1, 0)$	✗	✗	✓	$\emptyset$	$\emptyset$	
	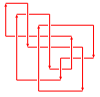	$(-1, 0)$ 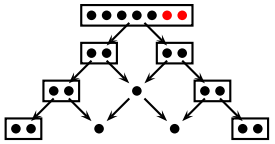	✓	✗?	✗?	$\emptyset$	$\emptyset$	
$m(9_{48})$	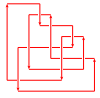	$(-8, 1)$ 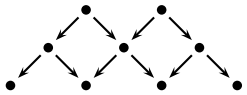	-	-	✓	-	-	

Knot Type	Grid Diagram	(tb, r)	$L = -L$?	$L = \mu(L)$?	$L = -\mu(L)$?	Ruling Invariant	Linearized Contact Homology	Note
9_{49}		$(3, 0)$	✓	✗?	✗?	$\emptyset$	$\emptyset$	
		$(3, 0)$	✓	✓	✓	$2z^2 + z^4$	$4 + t$	
	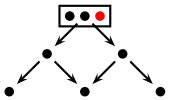							
$m(9_{49})$		$(-12, 1)$	-	-	✓	-	-	
	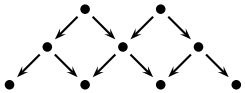							
10_{124}		$(7, 0)$	✓	✓	✓	$7 + 21z^2 + 21z^4 + 8z^6 + z^8$	$8 + t$	$T(3, 5)$
	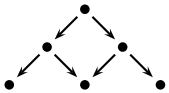							
$m(10_{124})$		$(-15, 2)$	-	-	✓	-	-	$T(3, -5)$
	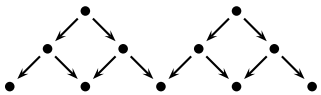							

Knot Type	Grid Diagram	(tb, r)	$L = -L$?	$L = \mu(L)$?	$L = -\mu(L)$?	Ruling Invariant	Linearized Contact Homology	Note
10_{128}	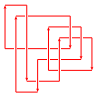	$(5, 0)$	✓	✗?	✗?	$2 + z^2$	$2t^{-2} + 2 + t + 2t^2$	
	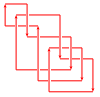	$(5, 0)$	✗?	✓	✗?	$2 + 6z^2 + 5z^4 + z^6$	$6 + t$	
	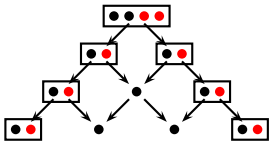							
$m(10_{128})$	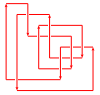	$(-14, 1)$	-	-	✓	-	-	
	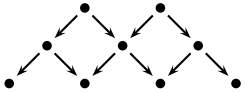							
10_{132}	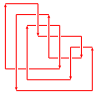	$(-8, 1)$	-	-	✓	-	-	
	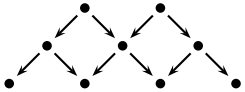							

Knot Type	Grid Diagram	(tb, r)	$L = -L$?	$L = \mu(L)$?	$L = -\mu(L)$?	Ruling Invariant	Linearized Contact Homology	Note
$m(10_{132})$		$(-1, 0)$	✗	✗	✓	$\emptyset$	$\emptyset$	
		$(-1, 0)$	✓	✓	✓	$\emptyset$	$\emptyset$	
	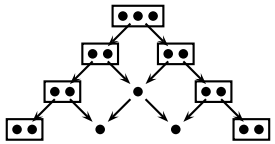							
10_{136}		$(-3, 0)$	✗	✗	✓	1	$t^{-2} + 2t^{-1} + 3t + t^2$	
		$(-3, 0)$	✓	✓	✓	1	$t^{-2} + 2t^{-1} + 3t + t^2$	
		$(-3, 0)$	✓	✗?	✗?	$1 + z^2$	$2t^{-1} + 2 + 3t$	
		$(-3, 0)$	✓	✗?	✗?	$1 + z^2$	$2t^{-1} + 2 + 3t$	
	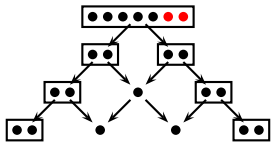							

Knot Type	Grid Diagram	(tb, r)	$L = -L$?	$L = \mu(L)$?	$L = -\mu(L)$?	Ruling Invariant	Linearized Contact Homology	Note
$m(10_{136})$	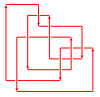 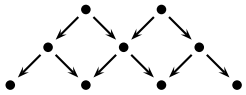	$(-6, 1)$	-	-	✓	-	-	
10_{139}	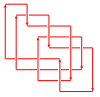 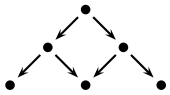	$(7, 0)$	✓	✓	✓	$6 + 21z^2 + 21z^4 + 8z^6 + z^8$	$8 + t$	
$m(10_{139})$	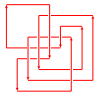	$(-16, 1)$	-	-	✓	-	-	
	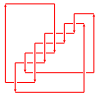 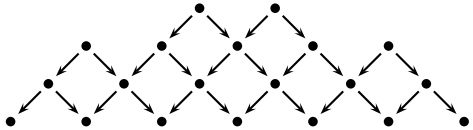	$(-17, 4)$	-	-	✓	-	-	
10_{140}	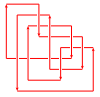 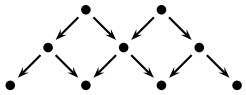	$(-8, 1)$	-	-	✓	-	-	

Knot Type	Grid Diagram	(tb, r)	$L = -L$?	$L = \mu(L)$?	$L = -\mu(L)$?	Ruling Invariant	Linearized Contact Homology	Note
$m(10_{140})$	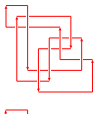	$(-1, 0)$	✗	✗	✓	1	t	
	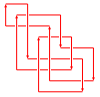	$(-1, 0)$	✓	✓	✓	1	t	
	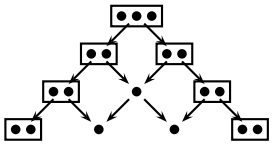							
10_{142}	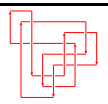	$(5, 0)$	✓	✓	✓	1	$3t^{-2} + t + 3t^2$	
	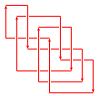	$(5, 0)$	✓	✓	✓	$1 + 6z^2 + 5z^4 + z^6$	$6 + t$	
	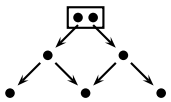							
$m(10_{142})$	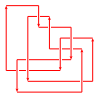	$(-14, 1)$	-	-	✓	-	-	
	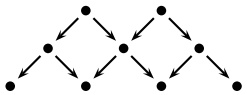							
10_{145}	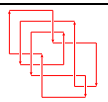	$(-12, 1)$	-	-	✓	-	-	
	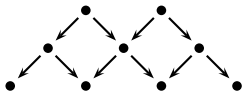							

Knot Type	Grid Diagram	(tb, r)	$L = -L$?	$L = \mu(L)$?	$L = -\mu(L)$?	Ruling Invariant	Linearized Contact Homology	Note
$m(10_{145})$	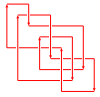	$(3, 0)$	✓	✓	✓	$2 + 4z^2 + z^4$	$4 + t$	
	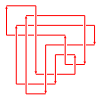	$(2, 1)$	-	-	✓	-	-	
	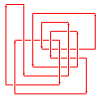	$(1, 0)$	✓	✓	✓	$\emptyset$	$\emptyset$	
	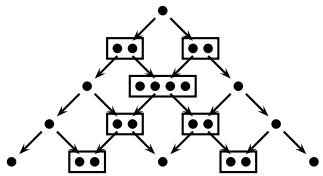							
10_{160}	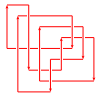	$(1, 0)$	✓	✗?	✗?	1	$2t^{-2} + t^{-1} + 2t + 2t^2$	
	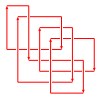	$(1, 0)$	✗?	✗?	✗?	$1 + 3z^2 + z^4$	$t^{-1} + 4 + 2t$	
	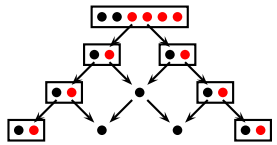							
$m(10_{160})$	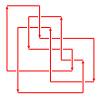	$(-10, 1)$	-	-	✓	-	-	
	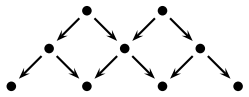							

Knot Type	Grid Diagram	(tb, r)	$L = -L$?	$L = \mu(L)$?	$L = -\mu(L)$?	Ruling Invariant	Linearized Contact Homology	Note
10_{161}	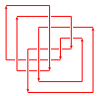	$(-14, 1)$	-	-	✓	-	-	
	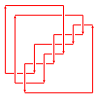	$(-15, 4)$	-	-	✓	-	-	
	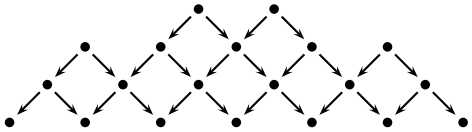							
$m(10_{161})$		$(5, 0)$	✓	✓	✓	$2 + 9z^2 + 6z^4 + z^6$	$6 + t$	
	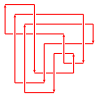	$(4, 1)$	-	-	✓	-	-	
	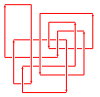	$(3, 0)$	✓	✓	✓	$\emptyset$	$\emptyset$	
	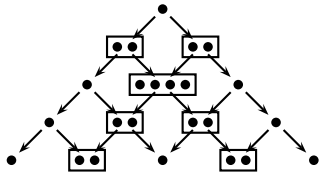							
$11n_{19}$	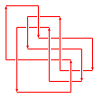	$(-8, 1)$	-	-	✓	-	-	
	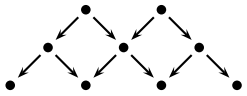							

Knot Type	Grid Diagram	(tb, r)	$L = -L$?	$L = \mu(L)$?	$L = -\mu(L)$?	Ruling Invariant	Linearized Contact Homology	Note
$m(11n_{19})$	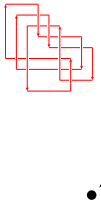	$(-1, 0)$	✓	✗?	✗?	$3 + 4z^2 + z^4$	$2t^{-1} + 4 + 3t$	
$11n_{38}$	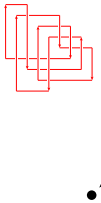	$(-5, 0)$	✓	✗?	✗?	$2 + z^2$	$3t^{-1} + 2 + 4t$	
$m(11n_{38})$	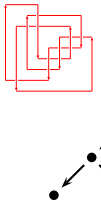	$(-4, 1)$	-	-	✓	-	-	
$11n_{95}$	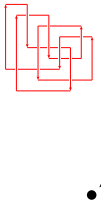	$(3, 0)$	✓	✗?	✗?	$3 + 6z^2 + 2z^4$	$4 + t$, $t^{-1} + 6 + 2t$	

Knot Type	Grid Diagram	(tb, r)	$L = -L$?	$L = \mu(L)$?	$L = -\mu(L)$?	Ruling Invariant	Linearized Contact Homology	Note
$m(11n_{95})$	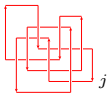	$(-12, 1)$	-	-	✗?	-	-	
	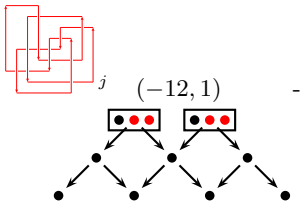	$(-12, 1)$	-	-	✓	-	-	
$11n_{118}$	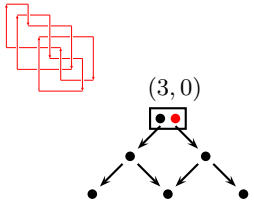	$(3, 0)$	✗?	✗?	✓	$4 + 7z^2 + 2z^4$	$4 + t,\ t^{-1} + 6 + 2t$	
$m(11n_{118})$	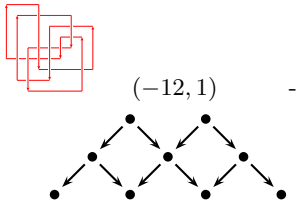	$(-12, 1)$	-	-	✓	-	-	
$12n_{242}$	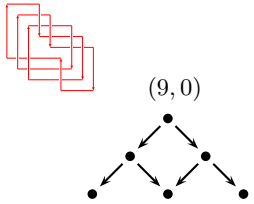	$(9, 0)$	✓	✓	✓	$9 + 39z^2 + 57z^4 + 36z^6 + 10z^8 + z^{10}$	$10 + t$	

Knot Type	Grid Diagram	(tb, r)	$L = -L$?	$L = \mu(L)$?	$L = -\mu(L)$?	Ruling Invariant	Linearized Contact Homology	Note
$m(12n_{242})$	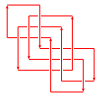	$(-18, 1)$	-	-	✓	-	-	
		$(-19, 4)$	-	-	✓	-	-	
	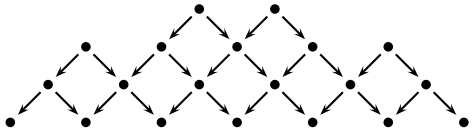							
$12n_{591}$	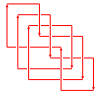	$(7, 0)$	✓	✓	✓	$4 + 17z^2 + 20z^4 + 8z^6 + z^8$	$8 + t$	
	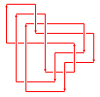	$(6, 1)$			✓			
	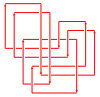	$(5, 0)$	✓	✓	✓	$\emptyset$	$\emptyset$	
	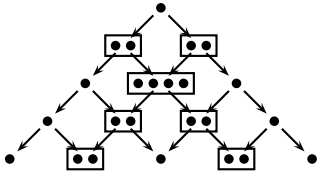							
$m(12n_{591})$	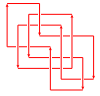	$(-16, 1)$	-	-	✓	-	-	
	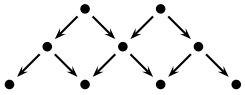							

Knot Type	Grid Diagram	(tb, r)	$L = -L$?	$L = \mu(L)$?	$L = -\mu(L)$?	Ruling Invariant	Linearized Contact Homology	Note
$15n_{41185}$	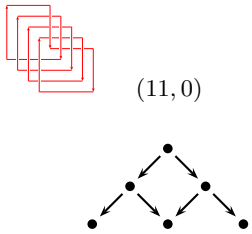	$(11, 0)$	✓	✓	✓	$14 + 70z^2 + 133z^4 + 121z^6 + 55z^8 + 12z^{10} + z^{12}$	$12 + t$	$T(4, 5)$
$m(15n_{41185})$	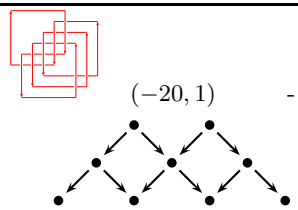	$(-20, 1)$	-	-	✓	-	-	$T(4, -5)$

Knot	Isotopy classes after S_+	Isotopy classes after S_-
$m(7_2)$	$L_1, L_2, -L_3 \mid L_3, L_4$	$L_1, L_2, L_3 \mid -L_3, L_4$
$m(7_6)$	$L_1, L_3 \mid L_2, -L_2, -L_3$	$L_1, -L_3 \mid L_2, -L_2, L_3$
9_{44}	$L_1, -\mu(L_1) \mid L_2, -\mu(L_3) : -\mu(L_2), L_3$	$-L_1, \mu(L_1) \mid -L_2, \mu(L_3) : \mu(L_2), -L_3$
$m(9_{45})$	$L_1, \mu(L_1), \mu(L_2) : -L_1, -\mu(L_1), L_2$	$L_1, \mu(L_1), L_2 : -L_1, -\mu(L_1), \mu(L_2)$
9_{48}	$L_1, L_3 \mid L_2, -L_2, -L_3, L_4, \mu(L_4)$	$L_1, -L_3 \mid L_2, -L_2, L_3, L_4, \mu(L_4)$
10_{128}	$L_1, -L_2 : \mu(L_1), L_2$	$L_1, L_2 : \mu(L_1), -L_2$
$m(10_{132})$	$L_1 \mid -L_1, L_2$	$L_1, L_2 \mid -L_1$
10_{136}	$L_1, L_4, \mu(L_4) \mid -L_1, L_2, L_3, \mu(L_3)$	$L_1, L_2, L_3, \mu(L_3) \mid -L_1, L_4, \mu(L_4)$
$m(10_{140})$	$L_1 \mid -L_1, L_2$	$L_1, L_2 \mid -L_1$
$m(10_{145})$	$S_-(L_1) \mid -L_2, L_3$	$S_+(L_1) \mid L_2, L_3$
10_{160}	$L_1, L_2, \mu(L_2) : \mu(L_1), -L_2, -\mu(L_2)$	$L_1, -L_2, -\mu(L_2) : \mu(L_1), L_2, \mu(L_2)$
$m(10_{161})$	$S_-(L_1) \mid -L_2, L_3$	$S_+(L_1) \mid L_2, L_3$
$12n_{591}$	$S_-(L_1) \mid -L_2, L_3$	$S_+(L_1) \mid L_2, L_3$

TABLE 2. Information about isotopy classes of Legendrian knots after stabilization. For each knot type, $L_1, L_2, \ldots$ denote the Legendrian knots depicted in the atlas, ordered from top to bottom. In this table, knots separated by commas can be shown to be Legendrian isotopic after one application of the appropriate stabilization. Vertical bars separate knots that are provably distinct after any number of the appropriate stabilizations; colons separate knots that the program conjectures are distinct after any number of stabilizations.

REFERENCES

[1] J. S. Birman and W. M. Menasco, Stabilization in the braid groups II: Transversal simplicity of knots, *Geom. Topol.* **10** (2006), 1425–1452 (electronic); arXiv:math/0310280.

[2] J. S. Birman and W. M. Menasco, A note on closed 3-braids, *Commun. Contemp. Math.* **10**, no. 1 supp., 1033–1047; arXiv:0802.1072.

[3] Y. Chekanov, Differential algebra of Legendrian links, *Invent. Math.* **150** (2002), no. 3, 441–483.

[4] W. Chongchitmate, Classification of Legendrian knots and links, Senior honors thesis, Duke University, 2010; available at `http://www.math.duke.edu/~ng/atlas/`.

[5] G. Civan, J. B. Etnyre, P. Koprowski, J. M. Sabloff, and A. Walker, Product structures for Legendrian contact homology, arXiv:0901.0490.

[6] M. Culler, Gridlink, available from `http://www.math.uic.edu/~culler/gridlink/`.

[7] T. Ekholm, J. Etnyre, L. Ng, and M. Sullivan, Filtrations on the knot contact homology of transverse knots, arXiv:1010.0450.

[8] Y. Eliashberg and M. Fraser, Topologically trivial Legendrian knots, *J. Symplectic Geom.* **7** (2009), no. 2, 77–127.

[9] J. B. Etnyre, Legendrian and transversal knots, in *Handbook of knot theory* (Elsevier, Amsterdam, 2005), 105–185; arXiv:math.SG/0306256.

[10] J. B. Etnyre and K. Honda, Knots and contact geometry I: torus knots and the figure eight knot, *J. Symplectic Geom.* **1** (2001), no. 1, 63–120; arXiv:math.GT/0006112.

[11] J. B. Etnyre and K. Honda, Cabling and transverse simplicity, *Ann. of Math. (2)* **162** (2005), no. 3, 1305–1333; arXiv:math/0306330.
[12] J. B. Etnyre and K. Honda, On connected sums and Legendrian knots, *Adv. Math.* **179** (2003), no. 1, 59–74; arXiv:math.SG/0205310.
[13] J. Etnyre, L. Ng, and V. Vértesi, Legendrian and transverse twist knots, arXiv:math/1002.2400.
[14] D. Fuchs, Chekanov-Eliashberg invariant of Legendrian knots: existence of augmentations, *J. Geom. Phys.* **47** (2003), no. 1, 43–65.
[15] G. T. Jin, H. Kim, and G.-S. Lee, Prime knots with arc index up to 10, in *Intelligence of low dimensional topology 2006*, *Ser. Knots Everything* **40** (2007), 65–74.
[16] T. Khandhawit and L. Ng, A family of transversely nonsimple knots, *Algebr. Geom. Topol.* **10** (2010), no. 1, 293–314.
[17] P. Lisca, P. Ozsváth, A. Stipsicz, and Z. Szabó, Heegaard Floer invariants of Legendrian knots in contact three–manifolds, arXiv:0802.0628.
[18] P. Melvin, J. Sabloff, et al., `Legendrian invariants.nb`, *Mathematica* program available at `http://www.haverford.edu/math/jsabloff/Josh_Sabloff/Research.html`.
[19] P. Melvin and S. Shrestha, The nonuniqueness of Chekanov polynomials of Legendrian knots, *Geom. Topol.* **9** (2005), 1221–1252; arXiv:math.GT/0411206.
[20] L. Ng, Legendrian mirrors and Legendrian isotopy, arXiv:math.GT/0008210.
[21] L. Ng, Computable Legendrian invariants, *Topology* **42** (2003), no. 1, 55–82; arXiv:math.GT/0011265.
[22] L. Ng, On arc index and maximal Thurston–Bennequin number, arXiv:math/0612356.
[23] L. Ng, Rational Symplectic Field Theory for Legendrian knots, *Invent. Math.*, to appear; arXiv:0806.4598.
[24] L. Ng, Combinatorial knot contact homology and transverse knots, arXiv:1010.0451.
[25] L. Ng, P. Ozsváth, and D. Thurston, Transverse knots distinguished by knot Floer homology, *J. Symplectic Geom.* **6** (2008), no. 4, 461–490; arXiv:math/0703446.
[26] L. Ng and D. Thurston, Grid diagrams, braids, and contact geometry, in *Proceedings of the 15th Gökova Geometry-Topology Conference*; arXiv:0812.3665.
[27] P. S. Ozsváth and A. Stipsicz, Contact surgeries and the transverse invariant in knot Floer homology, arXiv:0803.1252.
[28] P. S. Ozsváth, Z. Szabó, and D. P. Thurston, Legendrian knots, transverse knots and combinatorial Floer homology, *Geom. Topol.* **12** (2008), no. 2, 941–980; arXiv:math/0611841.
[29] P. Pushkar' and Y. Chekanov, Combinatorics of fronts of Legendrian links, and Arnol'd's 4-conjectures, *Uspekhi Mat. Nauk* **60** (2005), no. 1(361), 99–154.
[30] C. Shonkwiler and D. S. Vela-Vick, Legendrian contact homology and nondestabilizability, arXiv:0910.3914.

Mathematics Department, University of California at Los Angeles, Los Angeles, CA 90095

Mathematics Department, Duke University, Durham, NC 27708
URL: `http://www.math.duke.edu/~ng/`